which is determined by drain-source small-signal conductances. In the saturation region, such conductances are roughly proportional to I, which can be varied through V_{cQ} to make Q_I infinite, or of a given positive or negative value. In addition, assuming M1A and M1B operate as good source followers, varying I does not greatly affect the gate-source voltage of M2 (which determines g_m) and thus leaves ω_o practically unaffected as can be seen from eqn. 5 under the condition eqn. 2. Thus ω_o and Q_I can be tuned virtually independently of each other through $V_{c\omega}$ and V_{cQ}, respectively. This independence eases the design of the on-chip automatic tuning system that must generate $V_{c\omega}$ and V_{cQ}. Similar results can be obtained using a high-linearity crosscoupled version of the circuit in Fig. 2, or other related schemes.[4] In all cases, however, since V_{cQ} varies the operating point of several transistors, the worst-case output swing capability will be somewhat reduced compared to a circuit in which only $V_{c\omega}$ is varied. The reduction of swing is not as severe as when g_m must be tuned through the bias current in other schemes,[1,2] since there g_m varies as $\sqrt{I}$ and thus a large variation in I is needed. Here g_o varies roughly as I, and for practical cases the required range of I is not as large.

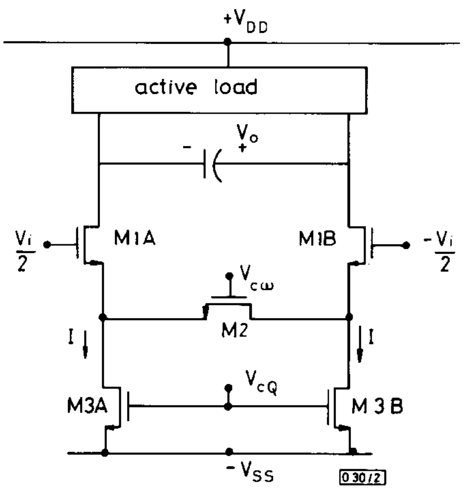

Fig. 2 *Linearised transconductance-capacitance integrator proposed in Reference 3*

Simulation results: The circuit of Fig. 2 was designed using active loads of the type employed in Reference 1, a load capacitance of 10 pF and power supply voltages of ± 5 V. To keep g_o small, and thus increase the frequency range over which high Q_I is maintained, channel lengths of $12\,\mu$m were used. The circuit was simulated using the program SPICE, with realistic model parameters. The near-independence in the tuning of ω_o and Q_I was verifiable. To check the capability of the circuit to maintain a high quality factor over a significant range of ω_o, the voltage $V_{c\omega}$ was set at three different values and in each case V_{cQ} was adjusted to make the phase $-90°$ ($Q_I = \infty$) at the corresponding ω_o. The results are shown in Fig. 3.

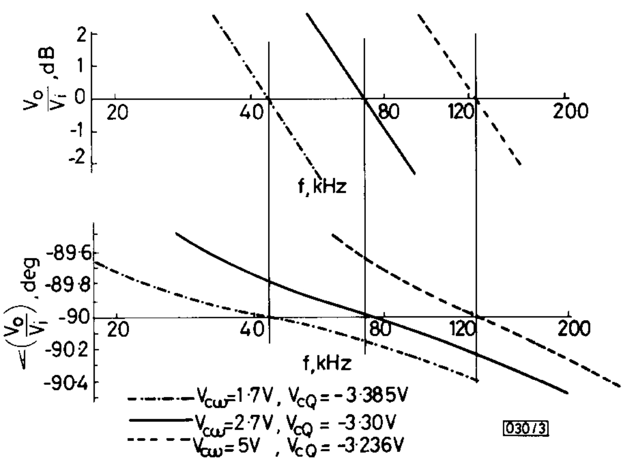

Fig. 3 *SPICE simulation results*

Conclusions: It has been shown that in a recently proposed transconductance-capacitance integrator one can tune the quality factor and the unity-gain frequency independently. This is accomplished by taking advantage of the same topological features that provide linearity without using additional components. The above tuning independence should make the integrator suitable for high-frequency, high-quality integrated filter design.

Z. CZARNUL*
Y. TSIVIDIS

7th July 1986

Department of Electrical Engineering and Center for Telecommunications Research
Columbia University
New York, NY 10027, USA

* On leave from the Institute of Electronic Technology, Technical University of Gdansk, Poland

References

1 KHORRAMABADI, H., and GRAY, P. R.: 'High-frequency continuous-time filters', *IEEE J. Solid-State Circuits*, 1984, **SC-19**, pp. 939–948
2 PARK, S. C., and SCHAUMANN, R.: 'Fully integrated analog filters in CMOS technology'. Proc. IEEE int. symposium on circuits and systems, 1986, pp. 1161–1164
3 TSIVIDIS, Y., CZARNUL, Z., and FANG, S. C.: 'MOS transconductors and integrators with high linearity', *Electron. Lett.*, 1986, **22**, pp. 245–246; Errata, *ibid.*, 1986, **22**, p. 619
4 CZARNUL, Z., and TSIVIDIS, Y.: 'MOS tunable transconductor', *ibid.*, 1986, **22**, pp. 721–722

SLOTTED ALOHA FOR MULTIHOP PACKET RADIO NETWORKS WITH MULTIPLE-DIRECTIONAL-ANTENNA STATIONS

Indexing terms: Telecommunications, Radio links

The slotted ALOHA protocol is modified to accommodate stations with multiple directional antennas in a multihop packet radio network environment. The one-hop throughput is derived for both the Poisson station distribution and the deterministic lattice station distribution. Numerical results show that the throughput values are very close for the two distributions. If the number of stations in the transmission circle is fairly large, say 50, the throughput gain using directional antennas could be as large as the number of directional antennas used.

Introduction: Chang and Chang[1] have examined the possible performance improvement of using directional transmitting antennas in a multihop packet radio network (PRN) environment. The protocols considered are slotted ALOHA and nonpersistent carrier-sense multiple access (CSMA). Each station is equipped with a single directional antenna. However, with a single directional antenna, there is a need to change the antenna directions for different receiving stations. To avoid this problem, we can use multiple directional antennas for transmission. In this letter we analyse the performance of slotted ALOHA with multiple directional antennas (SA/MDA) for deterministic and randomly distributed stations in a multihop PRN.

Let each station be equipped with m directional antennas for transmission. The broadcasting angle is 360°/m for each antenna and the orientation of the antennas is the same for all stations. We assume that all packets are of the same length and occupy one slot time. When a packet is ready, a station would choose a suitable antenna, depending on the location of the packet destination, and transmit the packet at the beginning of the next slot. If collision occurs, the station retransmits the packet after a random delay. Packet propagation delays are assumed to be negligible compared to the transmission time, and traffic acknowledgment is carried on a separate channel.

Analysis of SA/MDA:

(*a*) *Deterministic lattice distributed stations:* Let all stations be located on a lattice (see Fig. 1) and let the number of stations inside a circle of radius R (the transmission range) be N. At each station, let the probability of transmitting a packet at

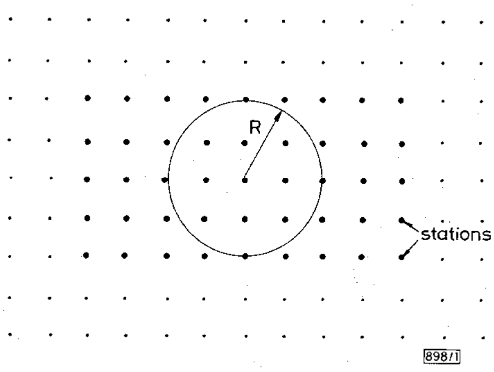

Fig. 1 *Deterministic lattice distribution of stations*

any particular slot be p, and let the traffic to all neighbouring stations be the same. Consider the transmission of a packet from P to Q, where Q is a neighbour of P. Let B be the event that this transmission is successful. We have

$$\text{prob}\,[B] = \text{prob}\,[\text{Q does not transmit}] \times \text{prob}\,[\text{all } N-2 \text{ neighbours of Q (excluding P) do not transmit toward Q's direction}]$$
$$= (1-p)(1-p/m)^{N-2} \qquad N > m \quad (1)$$

Define the one-hop throughput S as the average number of successful packet transmissions per slot from a station. We have

$$S = \text{prob}\,[\text{P transmits}] \times \text{prob}\,[B] = p(1-p)(1-p/m)^{N-2} \qquad N > m \quad (2)$$

For a given set of N and m, S is maximised by setting p to

$$p^* = \frac{2m}{(N-1) + 2m + \sqrt{[(N-1)^2 + 4m(m-1)]}} \quad (3)$$
$$= m/N \qquad \text{for } N \gg m$$

Substituting p^* into eqn. 2, we have

$$S = \frac{m}{N}\frac{1}{e} \qquad \text{for } N \gg m \quad (4)$$

Hence the throughput gain by using SA/MDA could be as much as the number of directional antennas used.

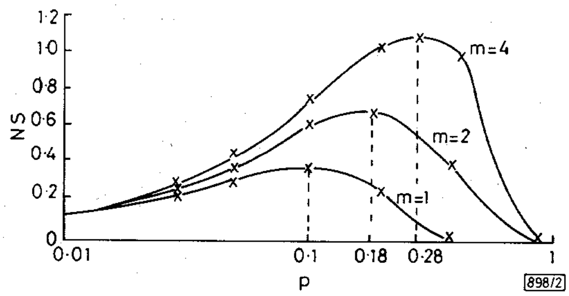

Fig. 2 *NS against p, lattice-distributed stations, N = 10*

(*b*) *Two-dimensional Poisson distributed stations:* Let λ be the average number of stations per unit area. Then $N \triangleq \lambda\pi R^2$ is the average number of stations in a circle of radius R. We adopt the most forward within R (MFR) routing strategy[2] and derive the throughput[3] as

$$S = (1 - e^{-N/2})p(1-p)\int_0^R \int_{-\pi/2}^{\pi/2} \exp\left(-\frac{p\lambda A'}{m}\right) \times f_{r,\theta}(r_0, \theta_0)\, d\theta_0\, dr_0 \quad (5)$$

where

$$A' = \pi R^2 - A_Z(r, \theta) \quad (6)$$

and

$$f_{r,\theta}(r_0, \theta_0) = \frac{\lambda r_0 \exp[-\lambda A_Z(r_0, \theta_0)]}{1 - e^{-N/2}} \quad (7)$$

is the joint probability density function of the locations of Q with respect to P in polar co-ordinates (r, θ). $A_Z(r, \theta)$ in eqn. 7 is the area of excluded region where no neighbours of Q can be located, and is given as[3]

$$A_Z(r, \theta) = R^2(\theta' - \sin 2\theta'/2) \quad (8)$$

where $\theta' = \cos^{-1}[(r/R)\cos\theta]$.

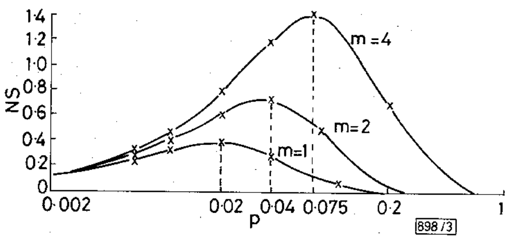

Fig. 3 *NS against p, lattice-distributed stations, N = 50*

Numerical results: Fig. 2 shows the total throughput in a circle of radius R (i.e. NS) as a function of transmission probability p for $m = 1$, 2 and 4. The stations are assumed to be located on a lattice and $N = 10$. Here we see that the optimum throughput values for $m = 1$, 2 and 4 have the ratio 1:1·8:2·9. Fig. 3 shows the same case but with $N = 50$; here the ratio is 1:1·92:3·64. Thus, for $N \gg 1$, the throughput gain could be as large as the number of directional antennas used.

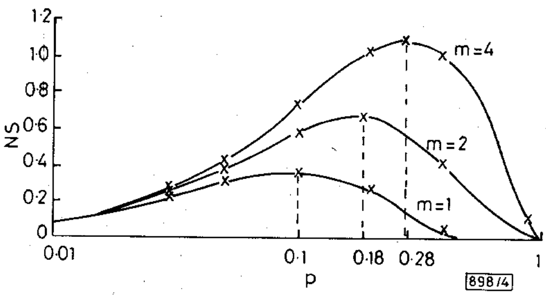

Fig. 4 *NS against p, Poisson-distributed stations, N = 10*

Figs. 4 and 5 show the same curves for Poisson-distributed stations. Compared with Figs. 2 and 3, the throughput values differ by no more than 6%. For $N = 50$, the throughput for the Poisson case is slightly higher, whereas for $N = 10$ the reverse is true.

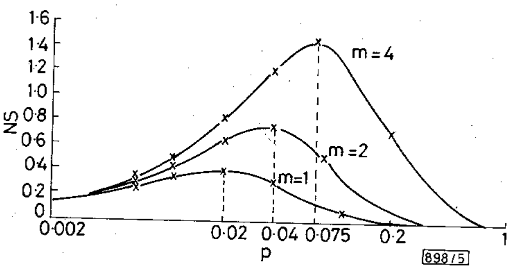

Fig. 5 *NS against p, Poisson-distributed stations, N = 50*

Thus we see that the one-hop throughput is quite independent of the spatial distribution of stations. Furthermore, as seen from the Figures, the optimum p values that maximise S are practically the same for the Poisson- and lattice-distributed station cases.

K.-W. HUNG
T.-S. YUM
Department of Electronics
Chinese University of Hong Kong
Shatin, NT, Hong Kong

5th June 1986

References

1 CHANG, J. F., and CHANG, C. J.: 'Optimal design parameters in a multihop packet radio network using random access techniques'. Proc. of GLOBECOM '84, Nov. 1984, pp. 493–497

2 TAKAGI, H., and KLEINROCK, L.: 'Optimal transmission ranges for randomly distributed packet radio terminals', *IEEE Trans.*, 1984, **COM-32**, pp. 246–257

3 HOU, T. C., and LI, V. O. K.: 'Performance analysis of routing strategies in multihop packet radio network'. Proc. of GLOBECOM '84, Nov. 1984, pp. 487–492

PHENOMENOLOGICAL APPROACH TO POLARISATION DISPERSION IN LONG SINGLE-MODE FIBRES

Indexing terms: Optical fibres, Polarisation

We describe a model for polarisation dispersion in single-mode fibres of arbitrary length and configuration that is based on the existence of principal states of polarisation. These are two orthogonal input states of polarisation whose corresponding output states exhibit zero dispersion in their state of polarisation to first order.

Introduction: Until now polarisation dispersion in single-mode fibres has played a negligible role in lightwave system design owing to the much more severe limitations imposed by chromatic dispersion. However, polarisation dispersion could become important in multigigabit systems where chromatic dispersion will by necessity be greatly reduced through the use of dispersion-shifted fibre and/or single-frequency lasers.[1] Its effect on future direct detection systems through pulse spreading and on coherent systems through both pulse spreading and depolarisation have yet to be fully assessed.

Experimental and theoretical work on polarisation dispersion in single-mode fibres has typically made use of a model in which two polarisation eigenmodes of the fibre are defined. The propagation constants for the two modes become distinct when the circular symmetry of the core is broken by stress or geometrically induced birefringence.[2] In real fibres the application of this model can become cumbersome when the fibre length exceeds ~ 1 km because mode coupling makes identification of the eigenmodes experimentally difficult.[3] Furthermore, when several fibre pieces are concatenated to form a long fibre length the random orientation of the birefringent axes of the various pieces make the application of such a model even less practical.

In this letter we propose a phenomenological model of polarisation dispersion for long fibre lengths. It is based on the observation that for any linear optical transmission medium that has no polarisation-dependent loss there exist orthogonal input states of polarisation for which the corresponding output states of polarisation are orthogonal and show no dependence on wavelength to first order. Such states have been observed in a 5 km piece of single-mode fibre.[4] We wish to generalise this observation and point out that these states of polarisation, which we call 'principal' states of polarisation, form a convenient basis set for the description and characterisation of polarisation dispersion in fibres of arbitrary length and configuration.

Existence of principal states of polarisation: To demonstrate the existence of principal states of polarisation, we consider a linear medium described by the complex transfer matrix $T(\omega)$. If we assume that there is no polarisation-dependent loss, then $T(\omega)$ takes the form

$$T(\omega) = e^{\beta(\omega)} U(\omega) \tag{1}$$

where $\beta(\omega)$ is in general complex and $U(\omega)$ is a unitary matrix:

$$U(\omega) = \begin{pmatrix} u_1(\omega) & u_2(\omega) \\ -u_2^*(\omega) & u_1^*(\omega) \end{pmatrix} \tag{2}$$

Here u_1 and u_2 satisfy the relation

$$|u_1|^2 = |u_2|^2 = 1$$

A monochromatic optical field $\vec{E}_a$, when transmitted by such a medium, produces an output field $\vec{E}_b$ given by

$$\vec{E}_b = T(\omega)\vec{E}_a \tag{3}$$

where ω is the optical frequency of the incident and transmitted fields. The complex field vectors $\vec{E}_{a,b}$ can be expressed in the form

$$\vec{E}_{a,b} = \begin{bmatrix} E^x_{a,b} \\ E^y_{a,b} \end{bmatrix} = \varepsilon_{a,b} e^{i\phi_{a,b}} \hat{\varepsilon}_{a,b} \tag{4}$$

where $\varepsilon_{a,b}$ and $\phi_{a,b}$ are the amplitudes and phases of the fields and $\hat{\varepsilon}_{a,b}$ are complex unit vectors specifying the states of polarisation.

In the presence of polarisation dispersion, which is one manifestation of the frequency dependence of the matrix $T(\omega)$, we may expect for an arbitrary but fixed input state of polarisation that the output polarisation state will vary with the frequency of the input wave. However, we wish to show here that for any medium described by $T(\omega)$ there exists at each frequency a set of two mutually orthogonal input states of polarisation for which the corresponding output states of polarisation are independent of frequency to first order.

To do this we start by taking the derivative of eqn. 3 with respect to frequency assuming a constant input field. This gives

$$\frac{d\vec{E}_b}{d\omega} = \frac{dT}{d\omega}\vec{E}_a = e^{\beta}[\beta' U + U']\vec{E}_a \tag{5}$$

The primes denote differentiation with respect to frequency. From eqn. 4 we have

$$\frac{d\vec{E}_b}{d\omega} = \left[\frac{1}{\varepsilon_b}\varepsilon_b' + i\phi_b'\right]\vec{E}_b + \varepsilon_b e^{i\phi_b}\frac{d\hat{\varepsilon}_b}{d\omega} \tag{6}$$

Combining eqns. 5 and 6 while making use of eqns. 1 and 3 leads to

$$\varepsilon_b e^{i\phi_b}\frac{d\hat{\varepsilon}_b}{d\omega} = e^{\beta}[U' - ikU]\vec{E}_a \tag{7}$$

where

$$k = \phi_b' + i\left[\beta' - \frac{1}{\varepsilon_b}\varepsilon_b'\right] \tag{8}$$

Since we wish to find the input states of polarisation that give zero dispersion in the output state, we set the left-hand side of eqn. 7 to zero, and look for solutions to the resulting eigenvalue equation:

$$[U' - ikU]\hat{\varepsilon}_a = 0 \tag{9}$$

We determine the allowed values of k in the usual manner by setting the determinant of the matrix in front of $\hat{\varepsilon}_a$ to zero. Making use of eqn. 2, this leads to the two solutions

$$k_\pm = \pm\sqrt{(|u_1'|^2 + |u_2'|^2)} \tag{10}$$

Inserting these two eigenvalues back into eqn. 9, we obtain the corresponding eigenvectors:

$$\hat{\varepsilon}_{a\pm} = e^{i\rho}\begin{bmatrix} \dfrac{[u_2' - ik_\pm u_2]}{D_\pm} \\ -\dfrac{[u_1' - ik_\pm u_1]}{D_\pm} \end{bmatrix} \tag{11}$$

where ρ is an arbitrary phase and

$$D_\pm = \sqrt{\{2k_\pm(k_\pm - \mathrm{Im}\,[u_1^* u_1' + u_2^* u_2'])\}} \tag{12}$$